A Modern Odyssey:
Quantum Gravity meets Quantum Collapse at Atomic and Nuclear physics energy scales in the Cosmic Silence

"SILICON DRIFT DETECTORS IN MODERN QUANTUM EXPERIMENTS: INVESTIGATING THE PAULI EXCLUSION PRINCIPLE"

Francesco Sgaramella
On behalf of VIP-2 (and SIDDHARTA-2) collaboration

INFN Istituto Nazionale di Fisica Nucleare
LABORATORI NAZIONALI DI FRASCATI

STRONG-2020

Silicon Drift Detectors (SDDs)

Thanks to their high energy and time resolution, SDDs are the ideal detectors for several types of experiments, from high energy physics (particle tracking) to nuclear and quantum physics (X-ray spectroscopy) and astrophysics.

Quantum mechanics

Silicon Drift Detectors

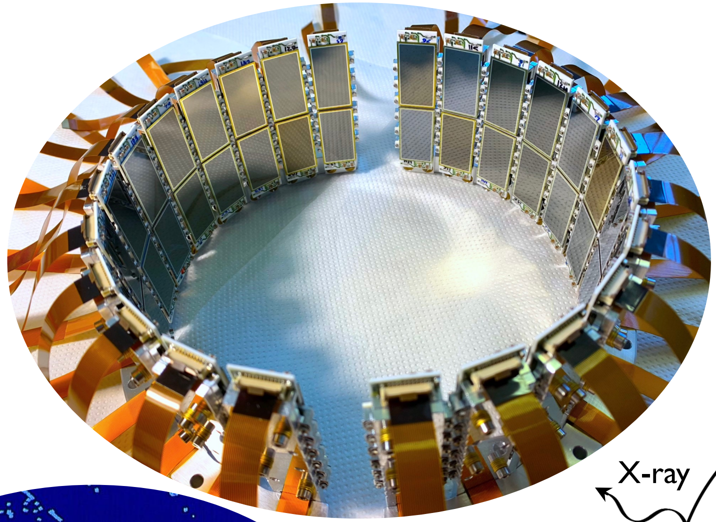

Astrophysics

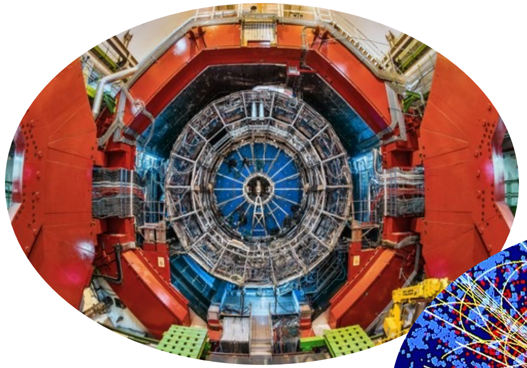

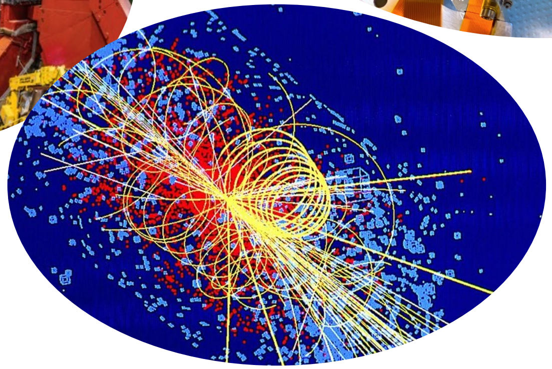

Particle and high energy physics

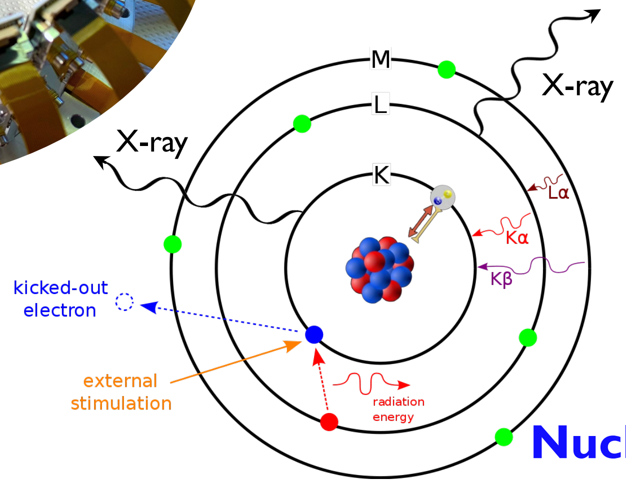

Nuclear-hadron physics

The Pauli Exclusion Principle

In an atom there cannot be two or more equivalent electrons for which the values of all four quantum numbers coincide. If an electron exists in an atom for which all of these numbers have definite values, then the state is occupied.

W.Pauli, Über den Zusammenhang des Abschlusses der Elektronengruppen im Atom mit der Komplexstruktur der Spektren, Zeitschrift für Physik 31 (1925) 765.

..The impression that the shadow of some incompleteness [falls] here on the bright light of success of the new quantum mechanics seems to me unavoidable.
W. Pauli, Nobel lecture 1945

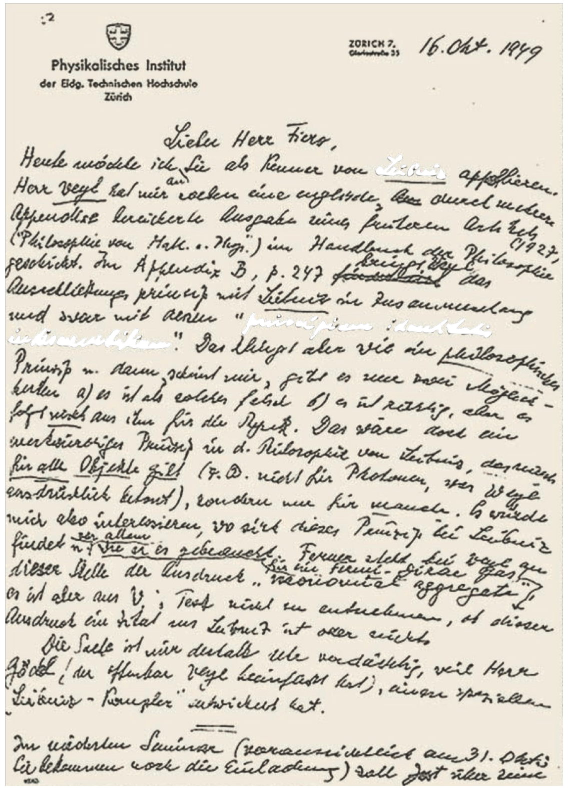
Physikalisches Institut
der Eidg. Technischen Hochschule
Zürich

ZÜRICH 7, 16. Okt. 1949

Lieber Herr Fierz,

Pauli Archive, holding: fierz_0092-064

The Pauli Exclusion Principle

Theories of Statistics Violation

O.W. Greenberg: AIP Conf.Proc.545:113-127,2004

"Possible external motivations for violation of statistics include: (a) violation of CPT, (b) violation of locality, (c) violation of Lorentz invariance, (d) extra space dimensions, (e) discrete space and/or time and (f) non-commutative spacetime......"

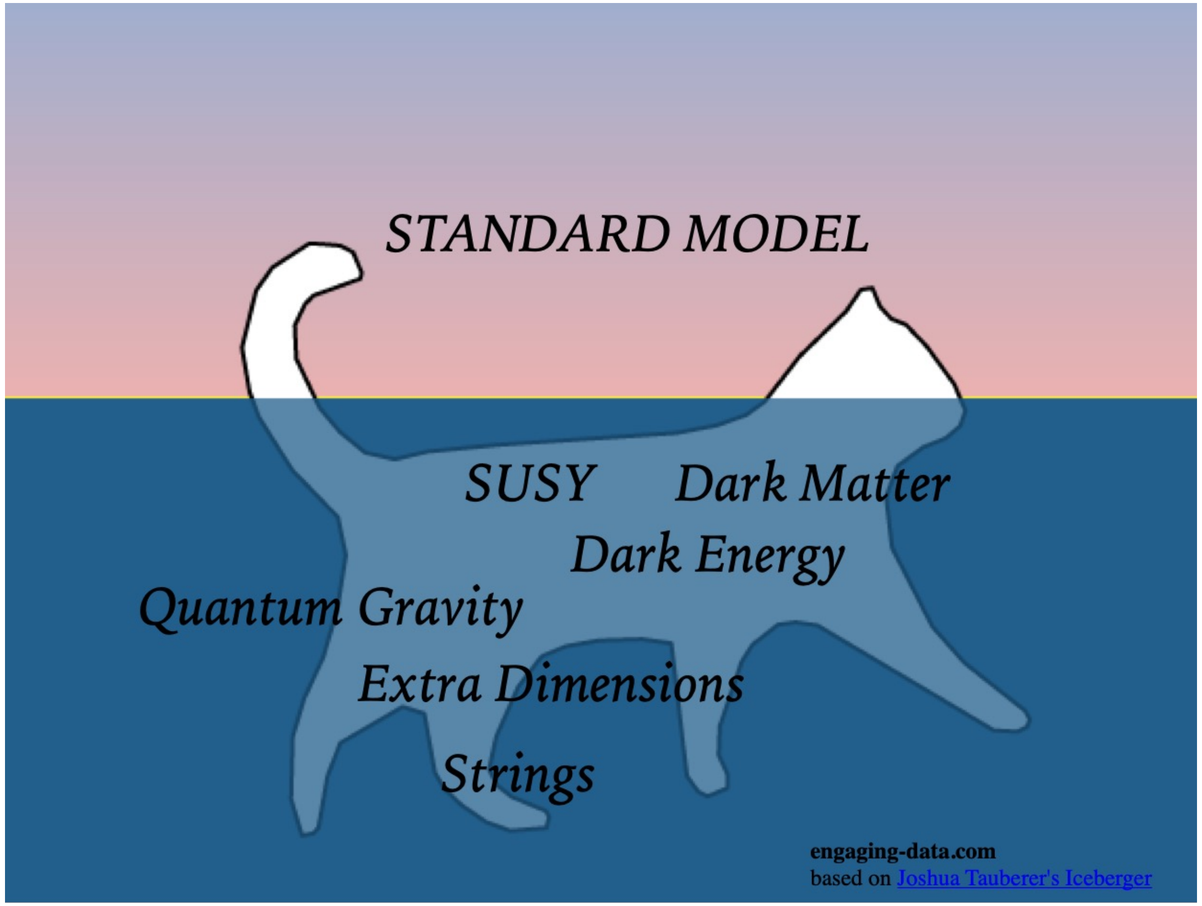

How to model the Pauli Exclusion Principle

- Ignatiev & Kuzmin model: Fermi oscillator with a third state

(Ignatiev, A.Y., Kuzmin, V. , Quarks '86: Proceedings of the 229 Seminar, Tbilisi, USSR, 1517 April 1986)

$$a^+|0\rangle = |1\rangle \qquad a|0\rangle = 0$$
$$a^+|1\rangle = \beta|2\rangle \qquad a|1\rangle = |0\rangle$$
$$a^+|2\rangle = 0 \qquad a|2\rangle = \beta|1\rangle$$

β quantifies the degree of violation in the transition

Open systems

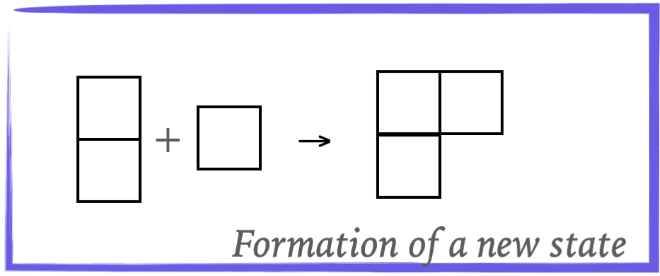

Two classes of PEP violation Models:

- **Deformation of commutation-anticommutation relations**
  Greenberg & Mohapatra: Local Quantum Field Theory, q parameter deforms anticommutators [Phys. Rev. Lett. 1987,59,2507]
  Subject to the **Messiah-Greenberg (M-G) Superselection Rule** - Can be tested in Open Systems only

- Space-time properties Balachandran, Addazi, Marcianò, Mavromatos-
  Not subject to the M-G rule - Can be tested in Closed Systems

Closed Systems

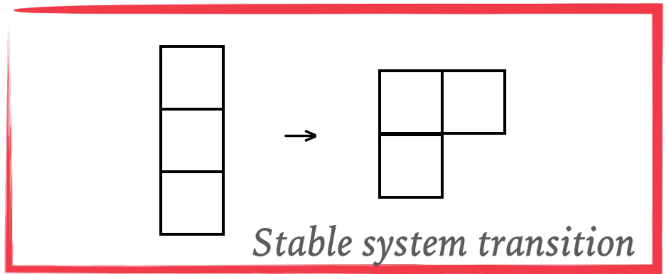

The Pauli Exclusion Principle in Open System

Greenberg, O. W. & Mohapatra, R. N., Phys Rev Lett 59, (1987).
E. Ramberg and G. A. Snow, Phys Lett B 238, 438-441(1990)

Search for anomalous electronic transitions in Cu
induced by a circulating current
introduced electrons interact with the valence electrons
search transition from 2p to 1s already filled by 2 electrons
alternated to X-ray background measurements without current

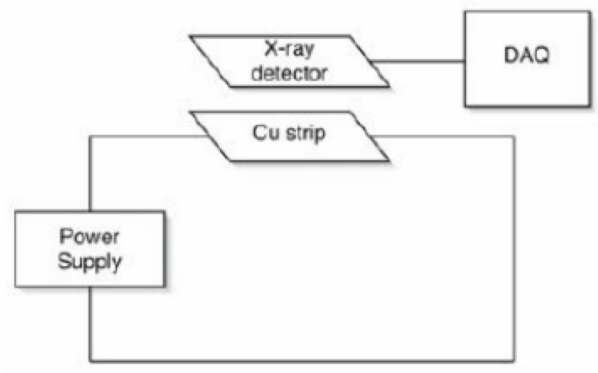

PEP Violation Signal

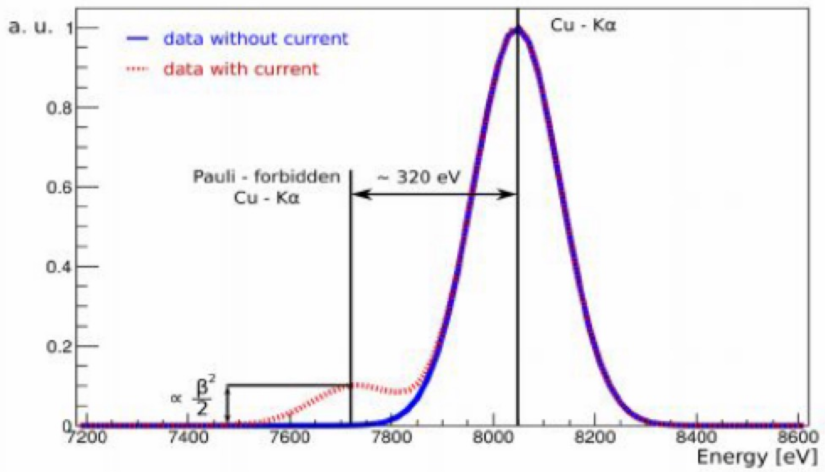

probability in terms of the number of electron-atom interactions, assuming a motion of the injected electrons subjected to a scattering length μ.

$$\beta^2/2 < 1.7 \times 10^{-26}$$

The Pauli Exclusion Principle in Open System

Search for anomalous X-ray transitions performed by electron introduced in a target trough a DC current (open system)

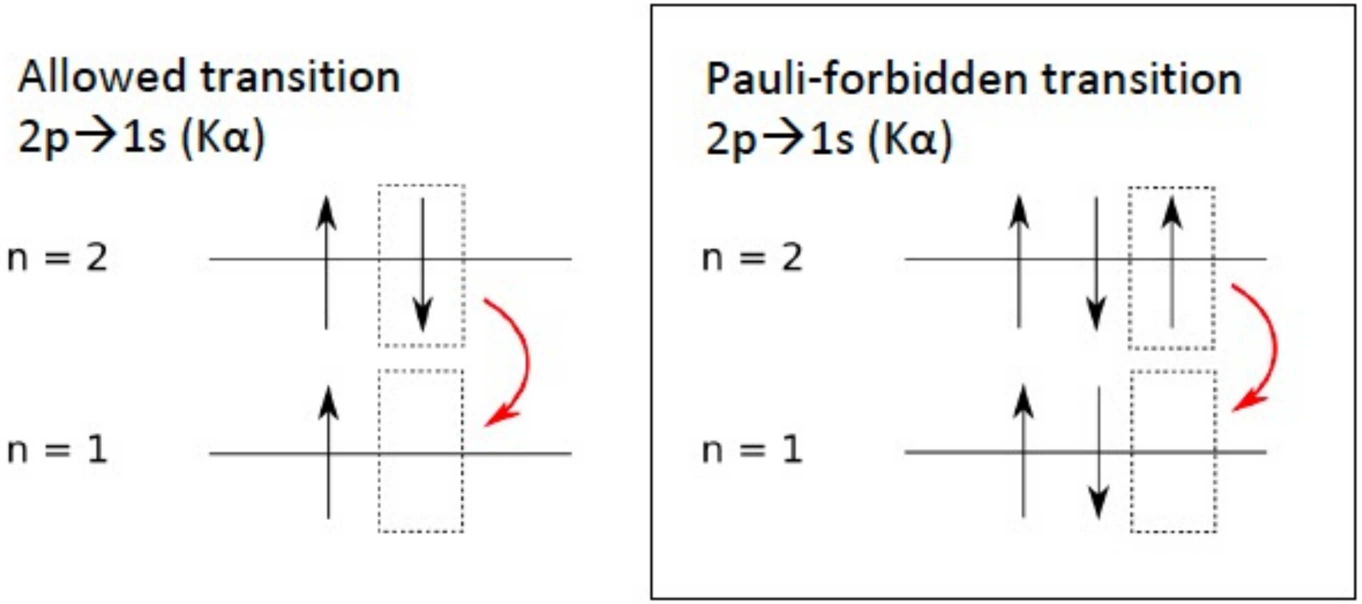

~ 8.05 keV in Cu

~ 7.7 keV in Cu

P. Indelicato (Ecole Normale Supérieure et Université Pierre et Marie Curie)
Multiconfiguration Dirac-Fock approach to account for the electron-screening effect

The VIP-2 Experiment

2 strip shaped Cu targets (25 um x 7 cm x 2 cm) more compact target
→ higher acceptance, thinner → **higher efficiency**
DC current supply to Cu bars

Cu strips cooled by a closed Fryka chiller circuit
→**higher current** (180 A peak current) @ 20 °C
of Cu target

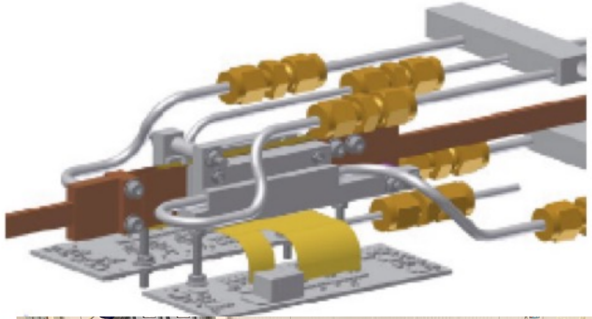

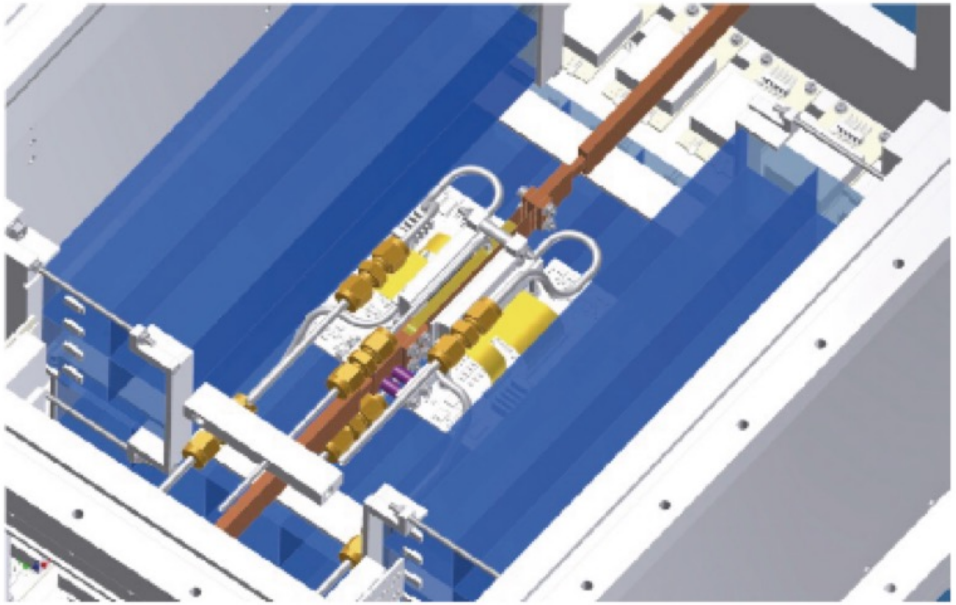

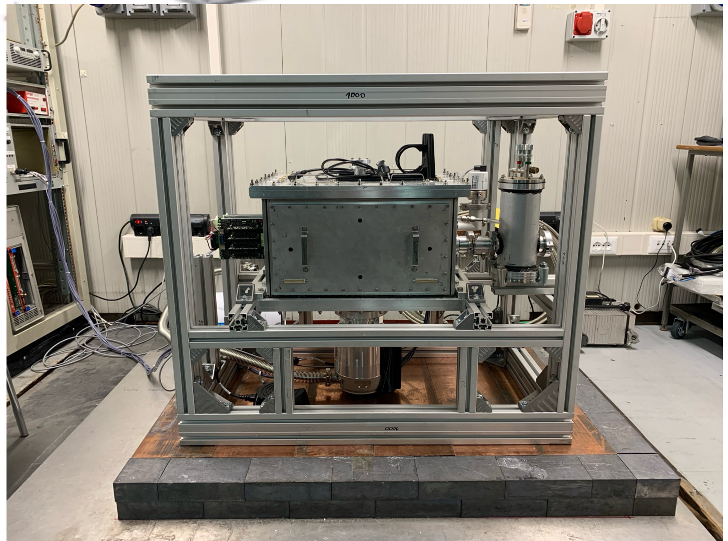

Silicon Drift Detectors – working principle

Developed by Gatti and Rehak (Gatti E. and Rehak P., Nucl. Instrum. Methods Phys. Res. 225, (1984), 608.) for particle tracking, nowadays are used to perform high precision X-ray spectroscopy thanks to their excellent energy and time resolutions

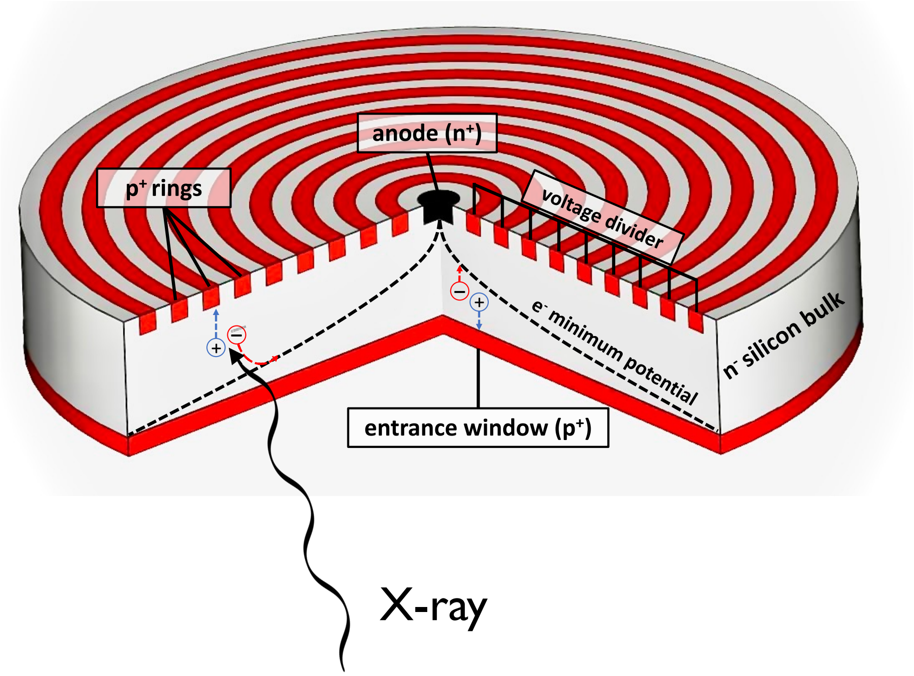

- Uniform entrance window → homogeneous sensitivity
- Large depleted region in which the electron-hole pairs, generated by the incident radiation, are separated through a reverse polarization field.
- A second electric field is superimposed to transport the electrons to the collection anode.
- Anode: small capacitance → large active area → reduced number of read-out channel

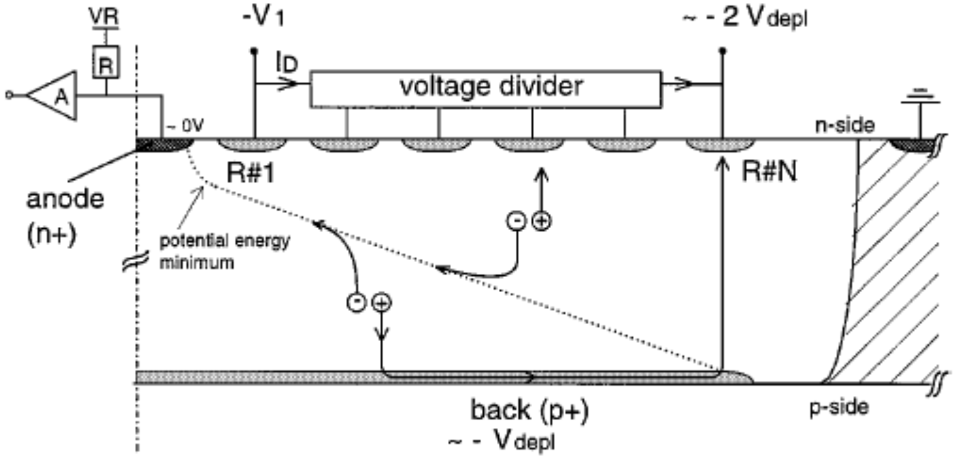

Silicon Drift Detectors

Large area Silicon Drift Detectors (SDDs) have been developed to perform high precision X-ray spectroscopy

INFN Istituto Nazionale di Fisica Nucleare Laboratori Nazionali di Frascati

FONDAZIONE BRUNO KESSLER FUTURE BUILT ON KNOWLEDGE

POLITECNICO MILANO 1863

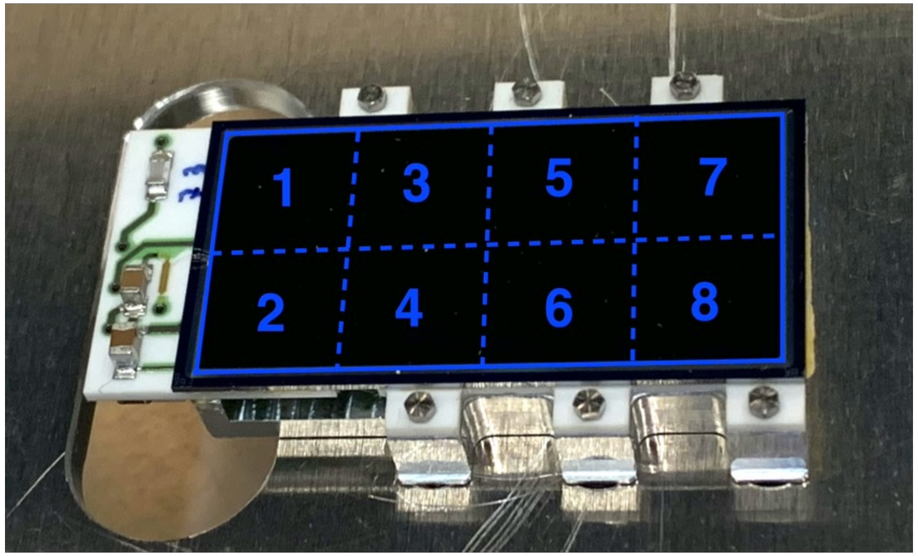

8 SDD units (0.64 cm^2)
for a total active area of 5.12 cm^2
Thickness of 450 μm ensures a high collection efficiency for X-rays of energy up to 10-12 keV

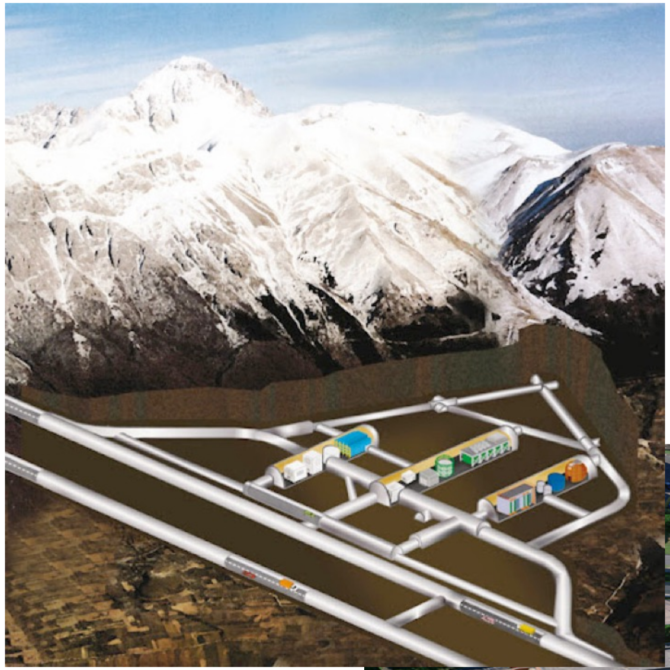

X-ray detector able to work in the cosmic silence of LNGS underground laboratories (PEP violation) as well as in a high radiation environment such as the DAFNE collider (kaonic atoms)

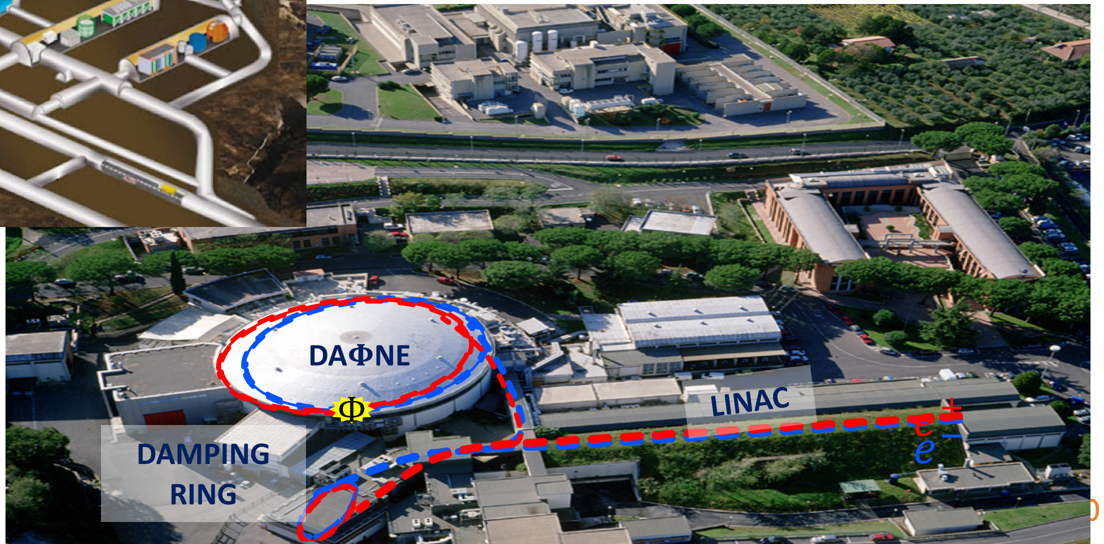

Silicon Drift Detectors

- Study and characterization of the SDDs energy and time response
- Front-end electronics based on the SFERA ASIC developed by PoliMi

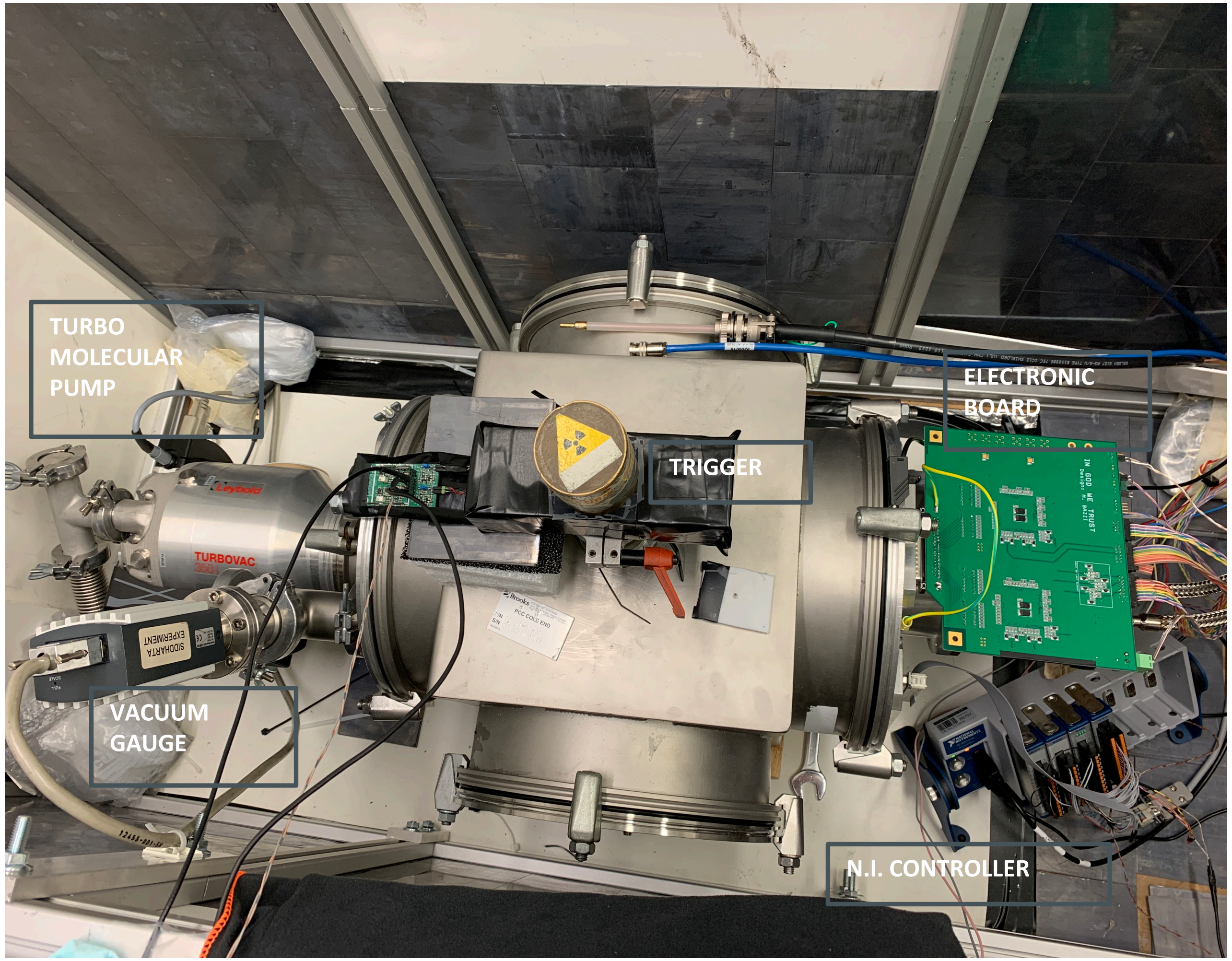

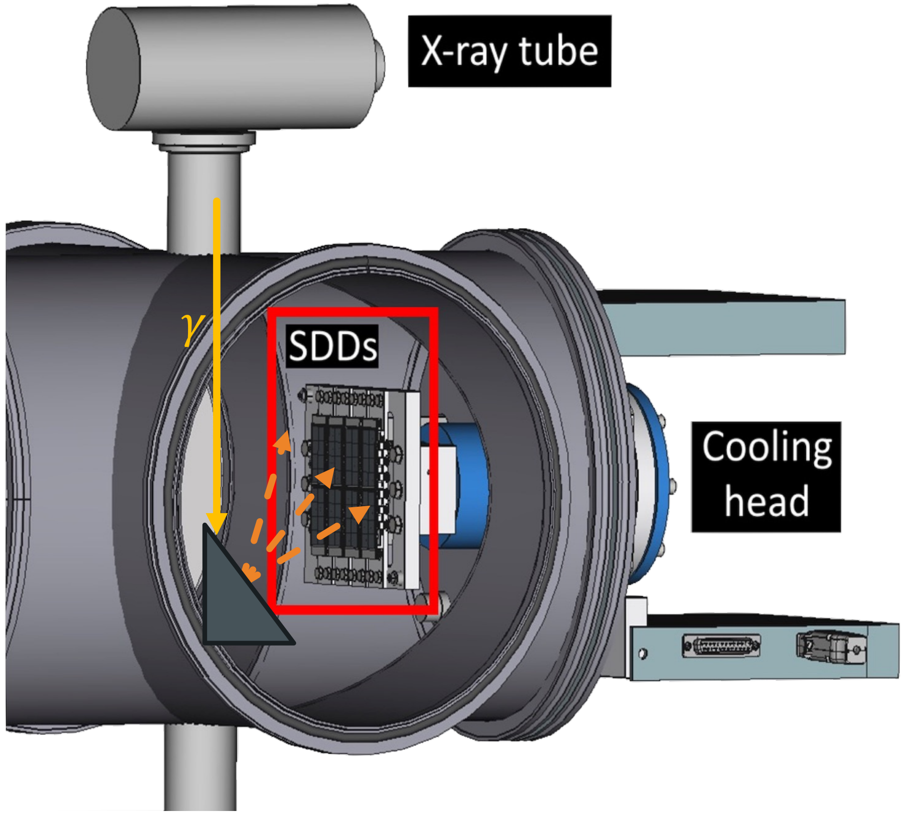

Silicon Drift Detectors

Energy response characterization

X-ray Tube used to induce the fluorescence emission of a multi element target made of Ti-Fe-Cu-Sr strips

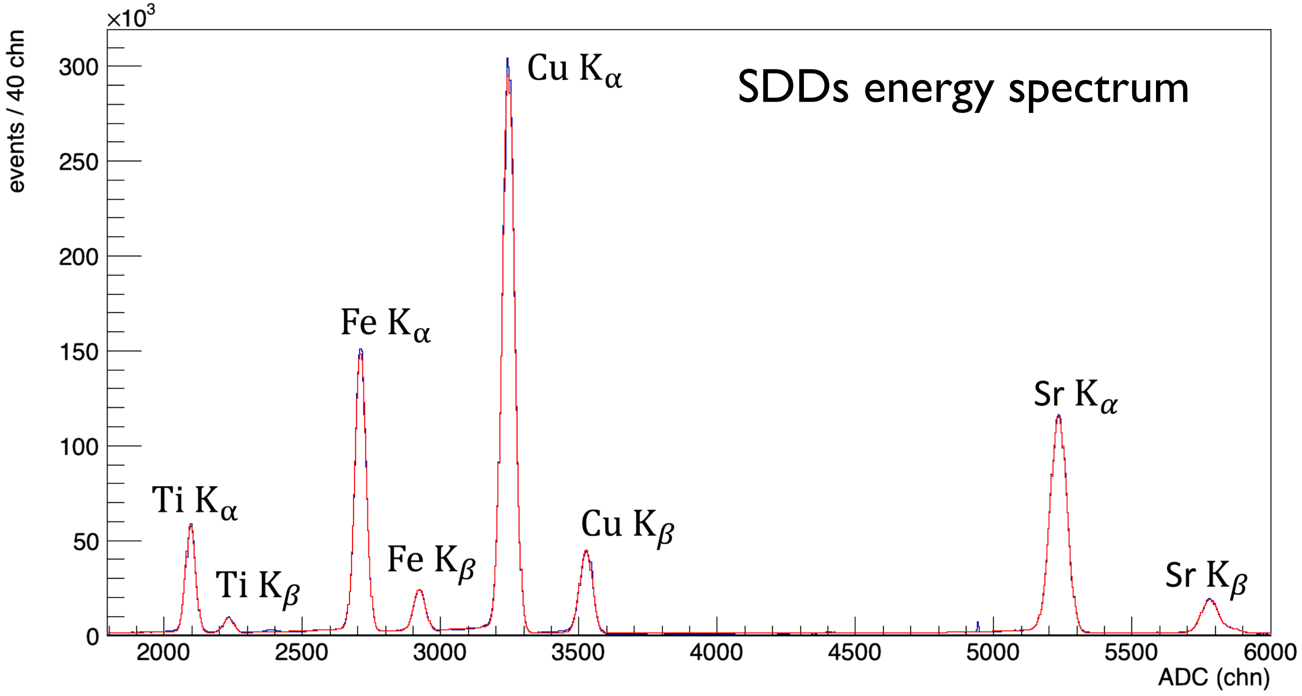

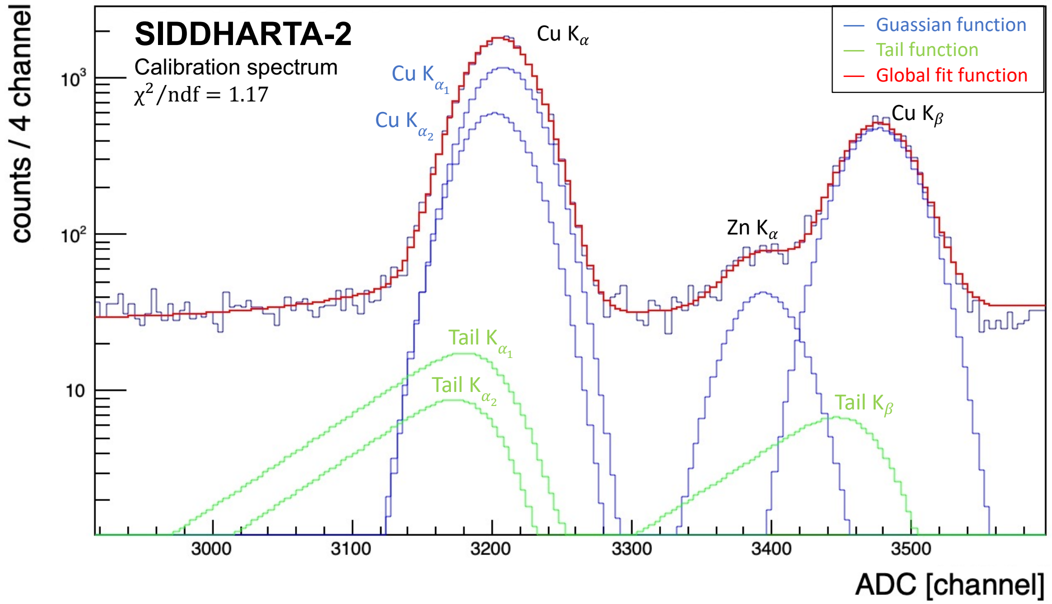

$$Gauss\ func.: H_G \cdot e^{\frac{-(x-x_0)^2}{2\sigma^2}}$$

$$\sigma = \sqrt{FF \cdot E \cdot \epsilon + \frac{noise^2}{2.35^2}}$$

$$Tail\ func.: H_T \cdot e^{\frac{x-x_0}{\beta\sigma}+\frac{1}{2\beta^2}} \cdot erfc\left(\frac{x-x_0}{\sqrt{2}\sigma}+\frac{1}{\sqrt{2}\beta}\right)$$

Silicon Drift Detectors spectroscopy response

The energy response is linear within few eV (<3 eV between 4 keV and 14 keV)
Excellent energy resolution @ 140 K

Linearity

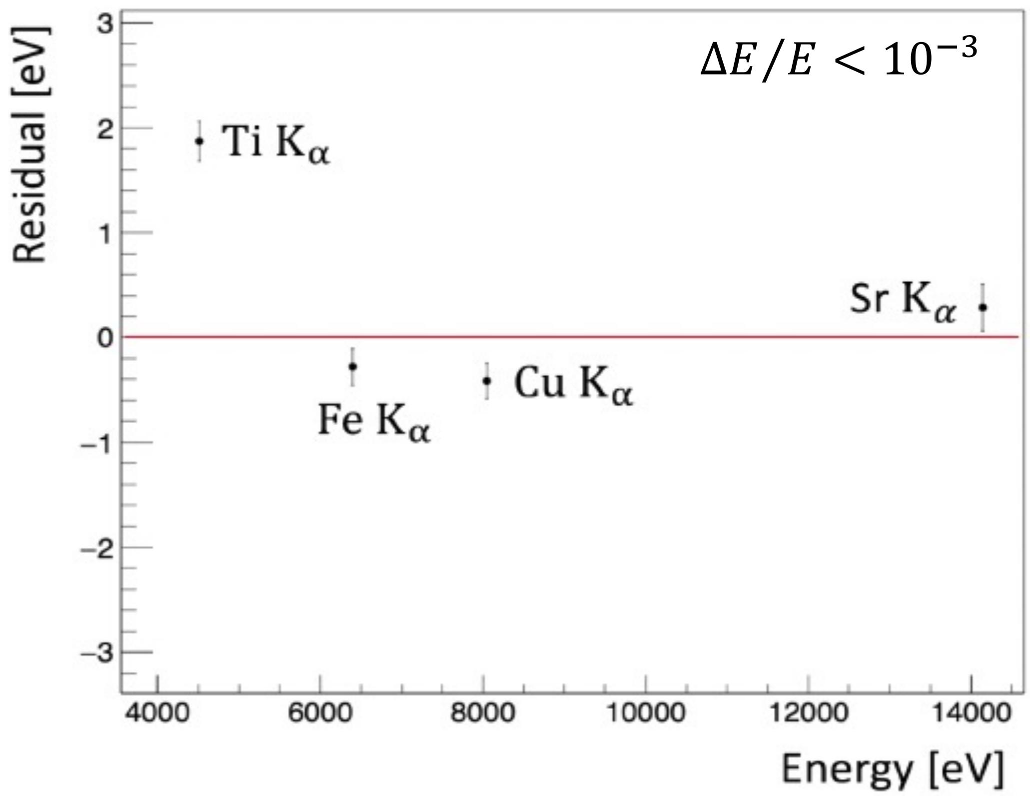

Energy resolution

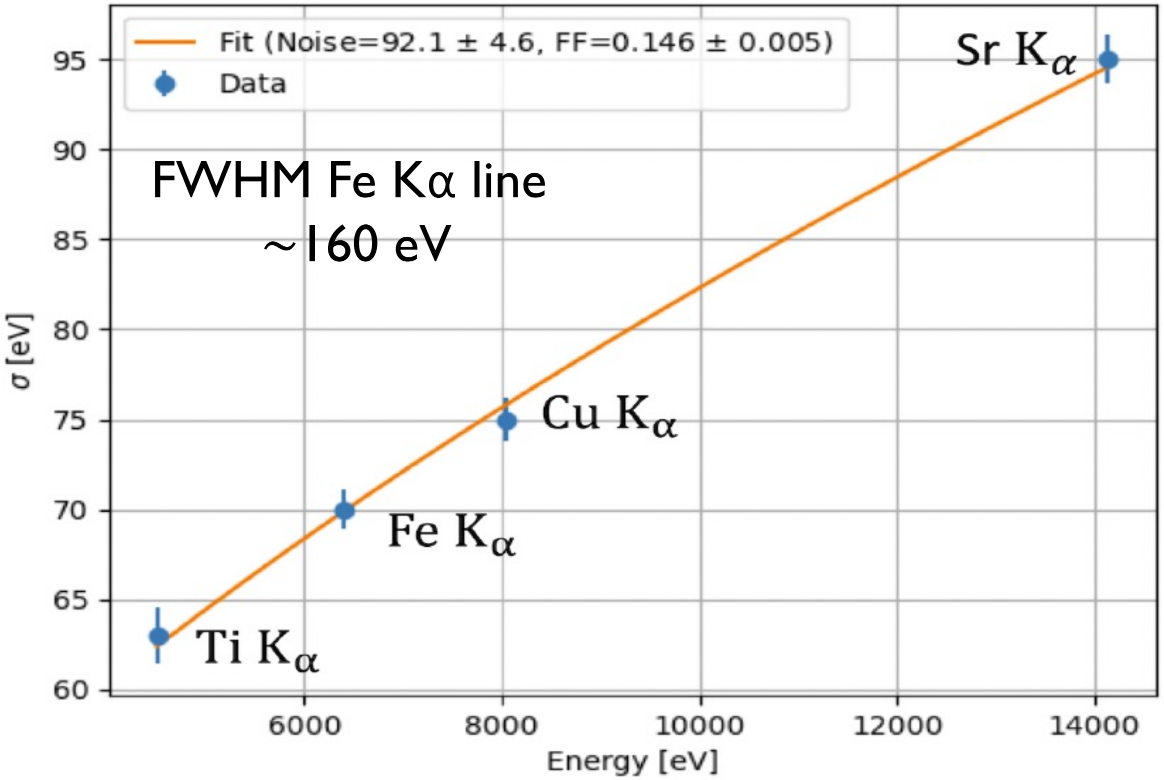

Miliucci M., Iliescu M., Sgaramella F., et al., 2022,Meas. Sci. Technol., 33 (9) 95502

Silicon Drift Detectors spectroscopy response

The energy response is linear within few eV (<3 eV between 4 keV and 14 keV)
Excellent energy resolution @ 140 K
Long term stability ~ eV

Stability

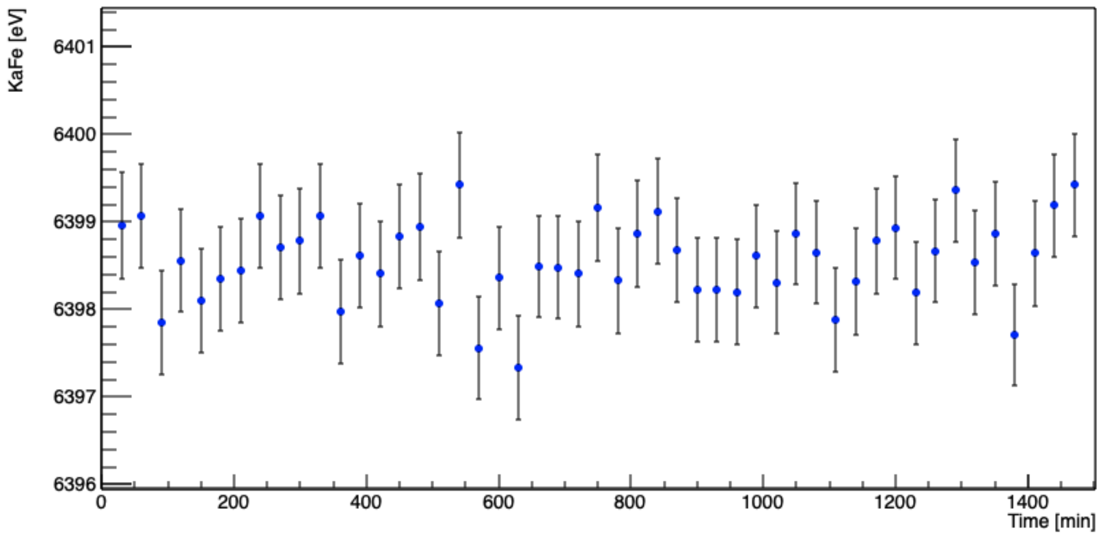

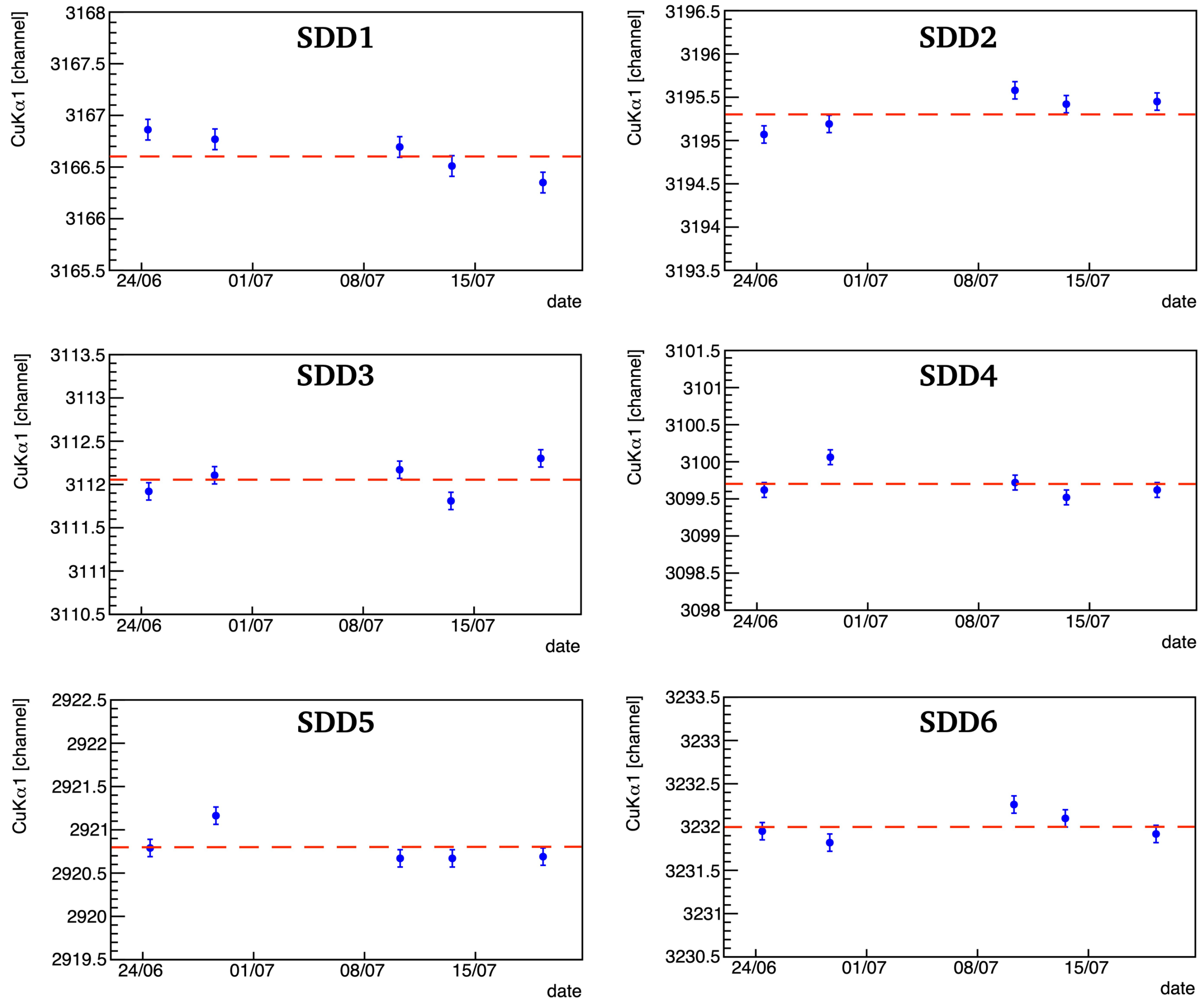

Silicon Drift Detectors spectroscopy response

SDDs spectroscopic response as function of the polarization voltage
Stable (~ eV) energy response in a wide range of polarization voltage

Linearity

$$r = \frac{\sqrt{\sum_{i=1}^{4}(P_i^{exp} - P^{label})^2}}{4}$$

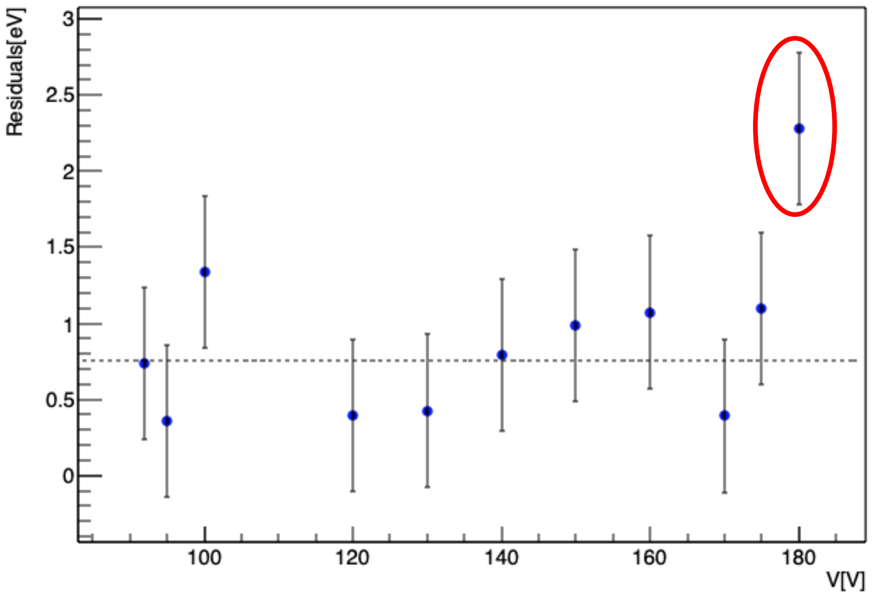

Energy resolution

$$FWHM_{TOT}^2 = FWHM_i^2 + FWHM_n^2 + FWHM_{c.c}^2$$

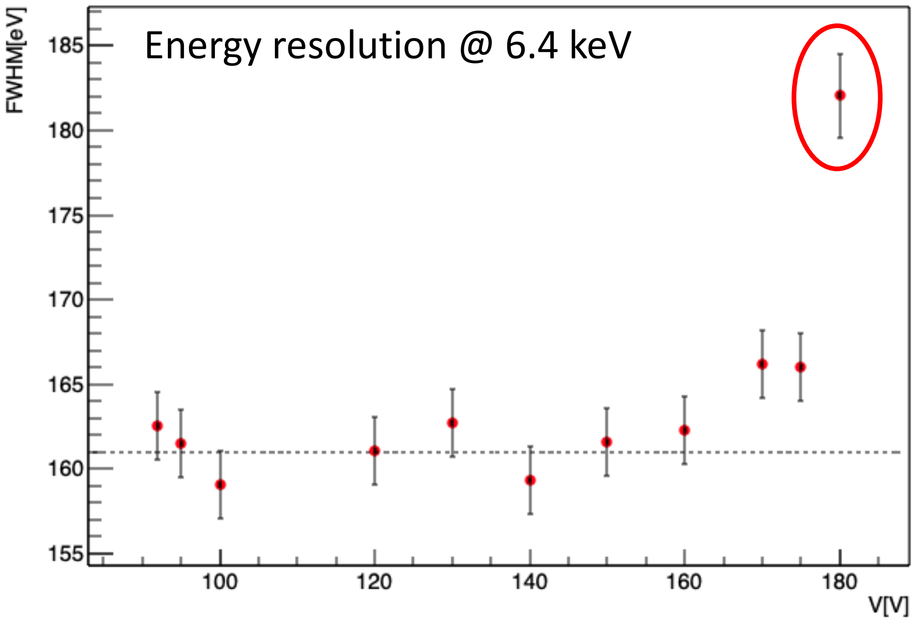

Silicon Drift Detectors spectroscopy response

SDDs spectroscopic response as function of the polarization voltage
Simulation used to study the electron drift path inside the SDD

Anode

HV = 140 V

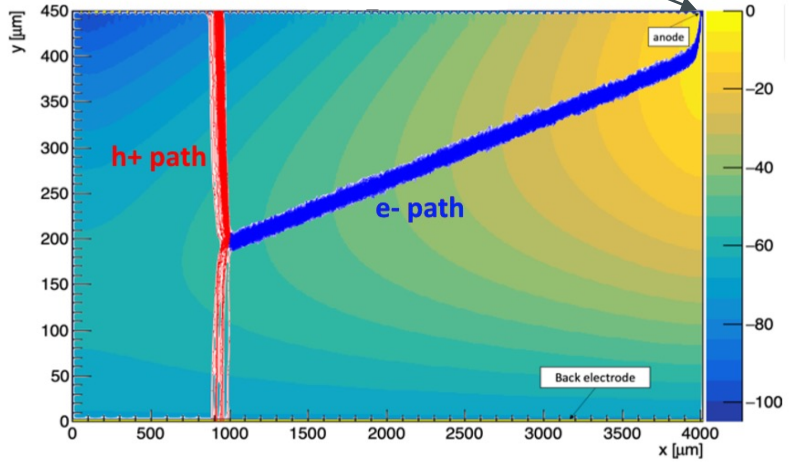

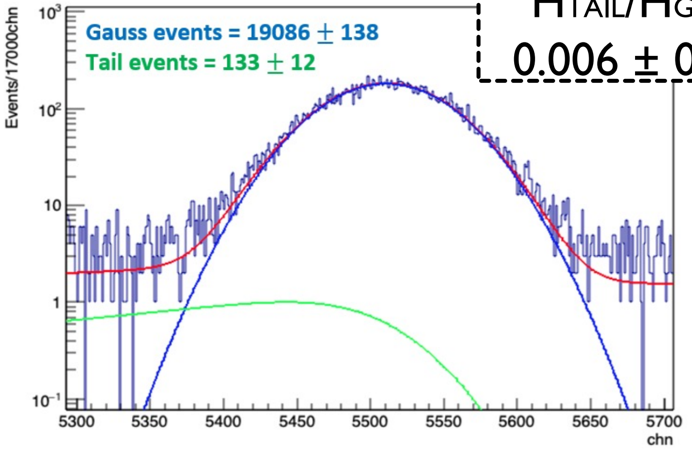

H_{TAIL}/H_{GAUSS}
0.006 ± 0.001

Anode

HV = 180 V

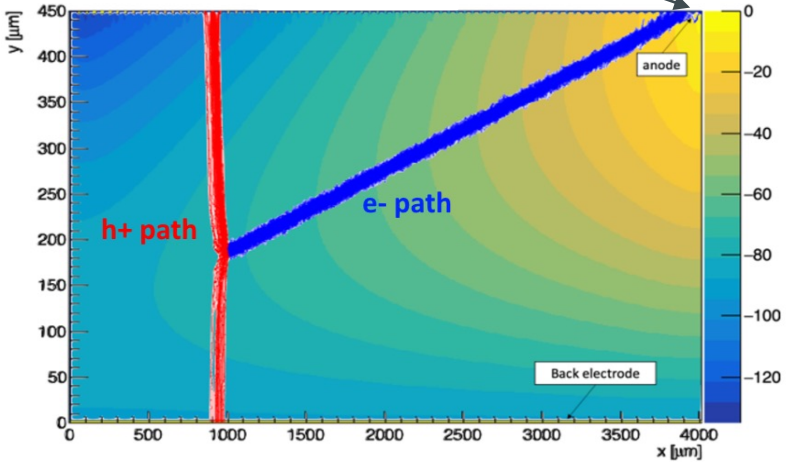

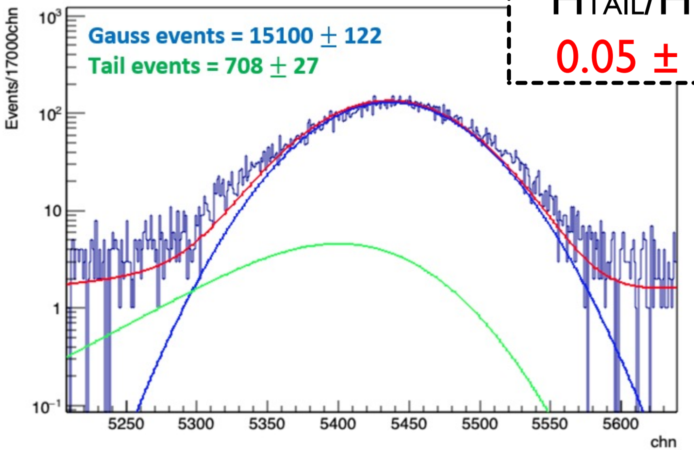

H_{TAIL}/H_{GAUSS}
0.05 ± 0.01

Silicon Drift Detectors

Time response characterization

The time response is defined as the time interval between the charge creation and its collection at the anode and depends on the drift velocity and the path length

$$t_{\text{drift}} = \frac{d}{v_{\text{drift}}} = \frac{d}{\mu \cdot E}$$

Given the small transverse distance (20 times smaller than the SDD side) the main contribution to the collection path d is the radial distance from the generation point to the anode

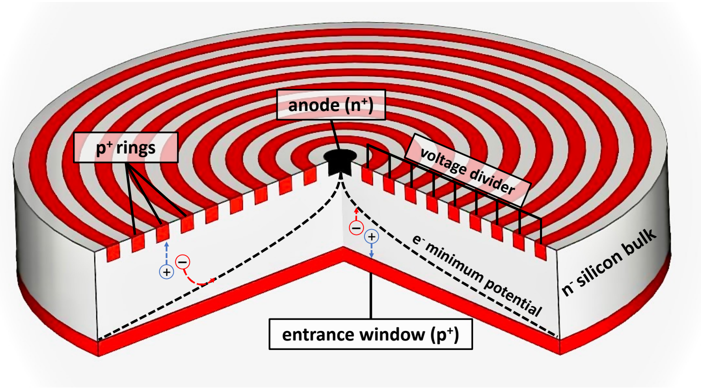

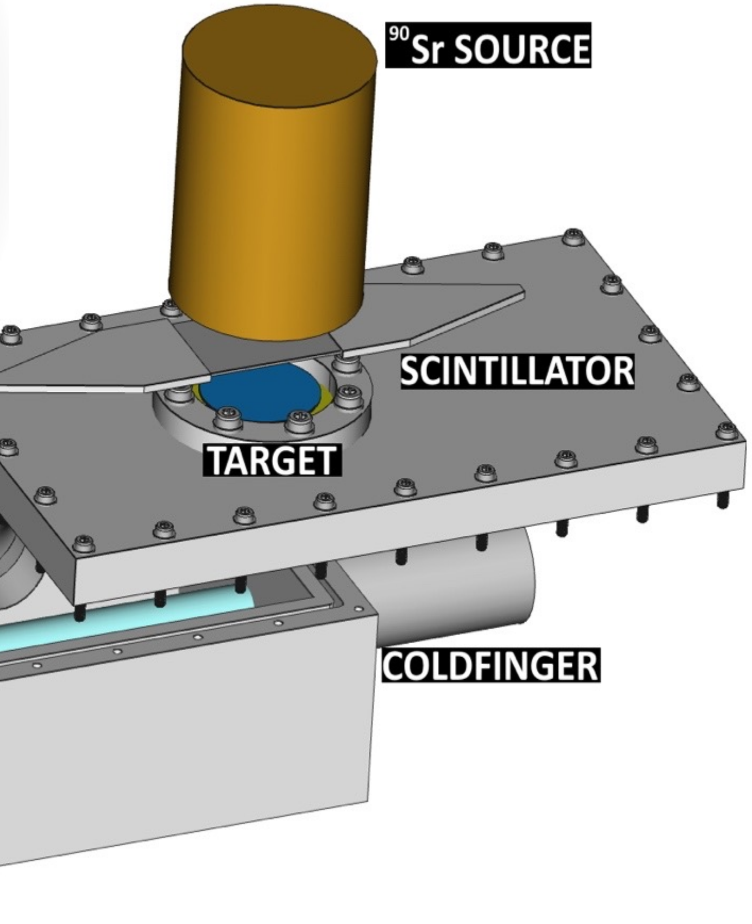

Silicon Drift Detectors

Study of the time resolution as function of the SDDs temperature
(polarization voltage -140 V)

Energy spectrum

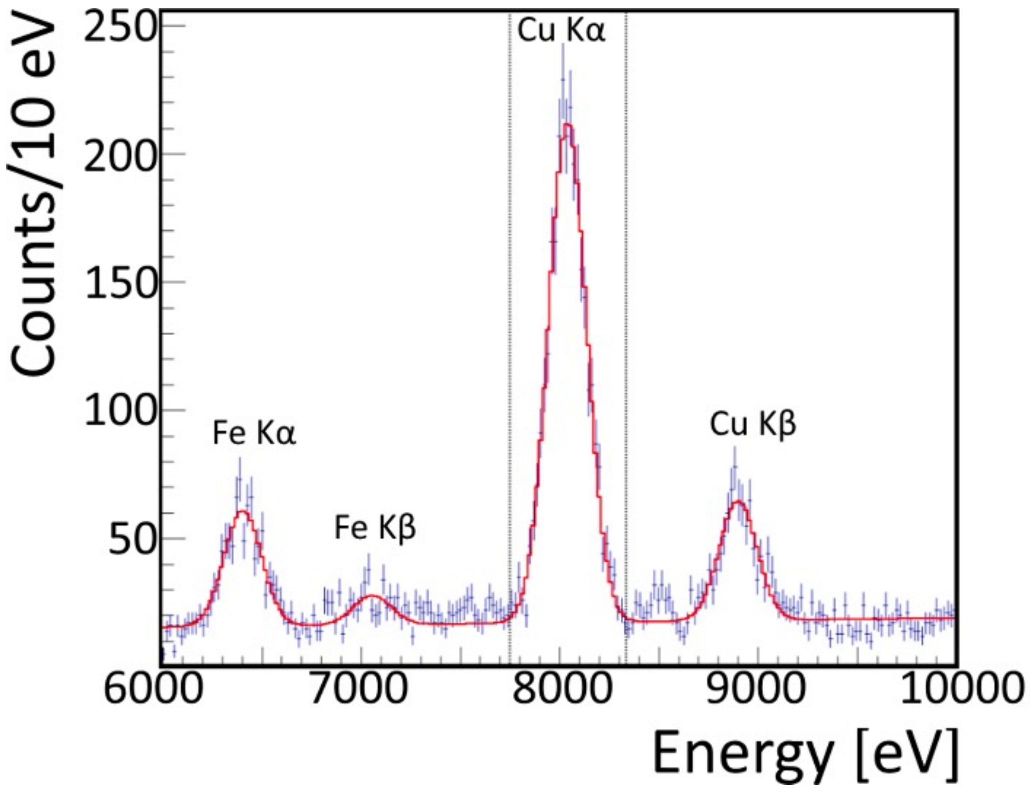

Time distribution of Cu K_α peak

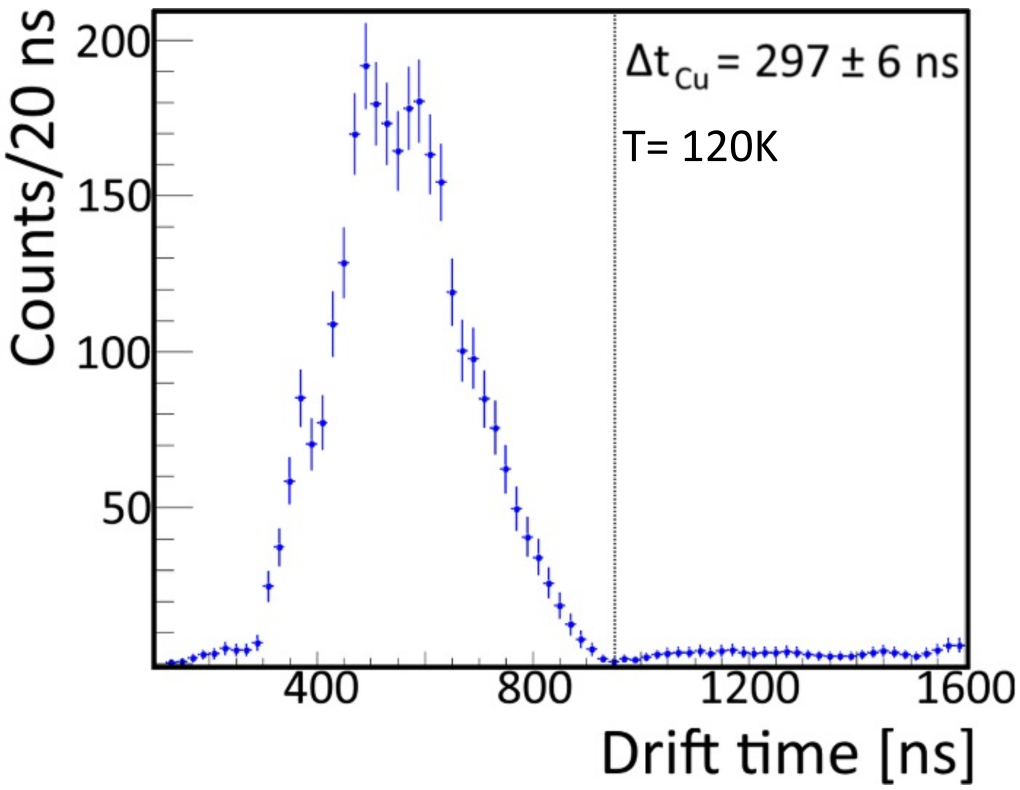

Silicon Drift Detectors

Study of the time resolution as function of the SDDs temperature (polarization voltage -140 V)

Summary of the SDD timing response at different temperatures: ±20 ns variation to the 3σ threshold defines the systematic errors.

Temperature (K)	δT (K)	Entries	Δt Cu Kα (ns)	Stat. (ns)	Syst. (+) (ns)	Syst. (−) (ns)
100.0	0.2	2996	250	5	2	−1
107.3	0.1	2327	273	6	0	−1
119.8	0.2	2907	297	6	1	0
127.5	0.3	2976	332	6	1	−1
138.3	0.2	3076	361	7	1	−1
147.5	0.2	1585	400	10	1	−1
157.8	0.2	2358	435	9	2	−2
178.8	0.4	2870	556	10	1	−1
198.1	0.2	3590	761	13	0	0

Miliucci M., Iliescu M., Sgaramella F., et al., 2022,Meas. Sci. Technol., 33 (9) 95502

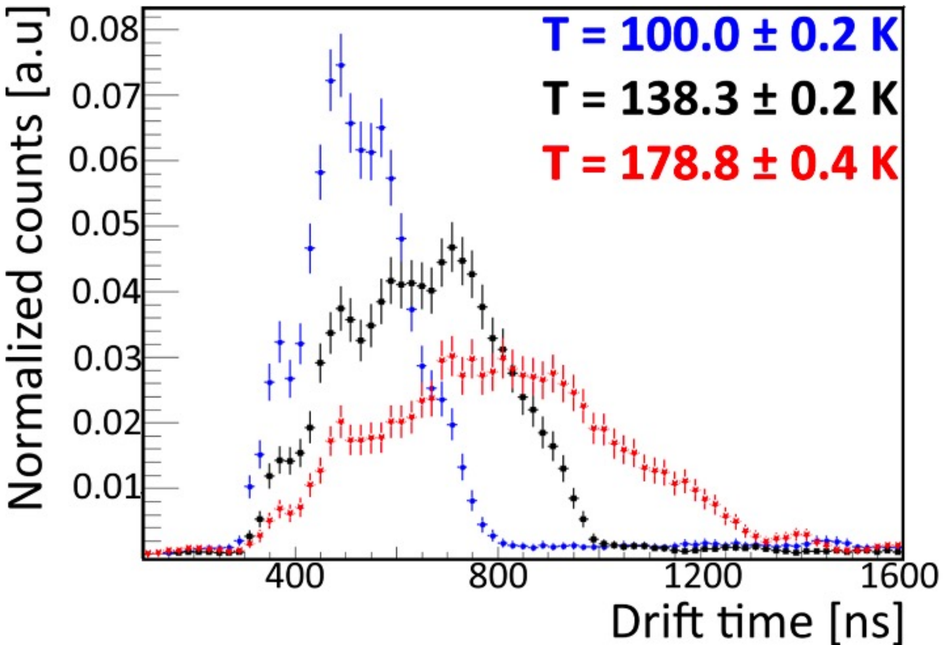

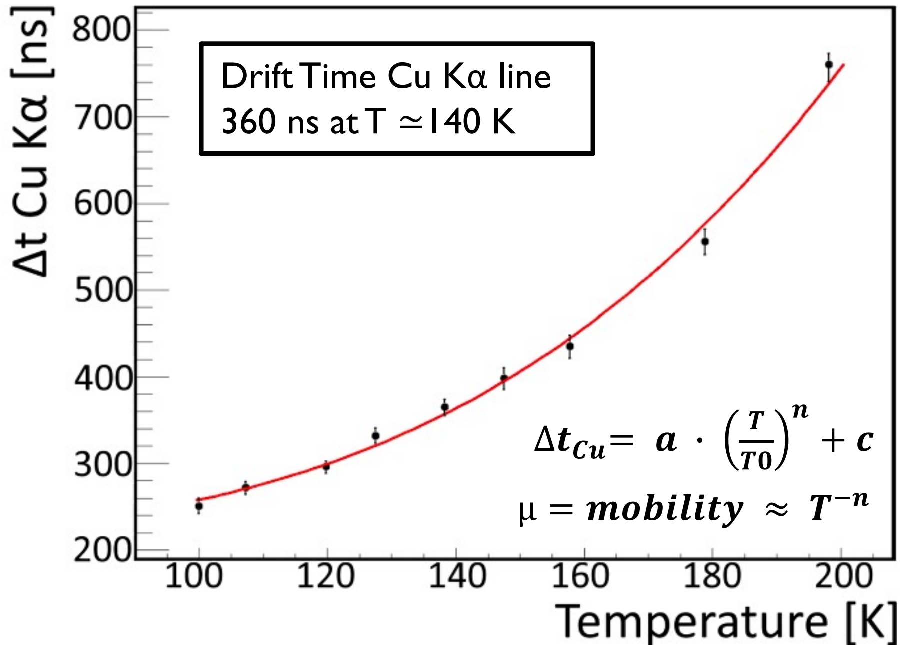

The VIP-2 Experiment

Silicon Drift Detectors (**SDDs**) higher resolution (176 eV FWHM at 8 →keV), faster (triggerable) detectors. 4 arrays of 2 x 4 SDDs 8mm x 8mm each, cooled down to - 140 °C

Calibrated with 55Fe and Ti target: novel Machine Learning and differentiable programming techniques to enhance the energy resolution (*F. Napolitano et al 2024 Meas. Sci.Technol.* ***35*** *025501*)

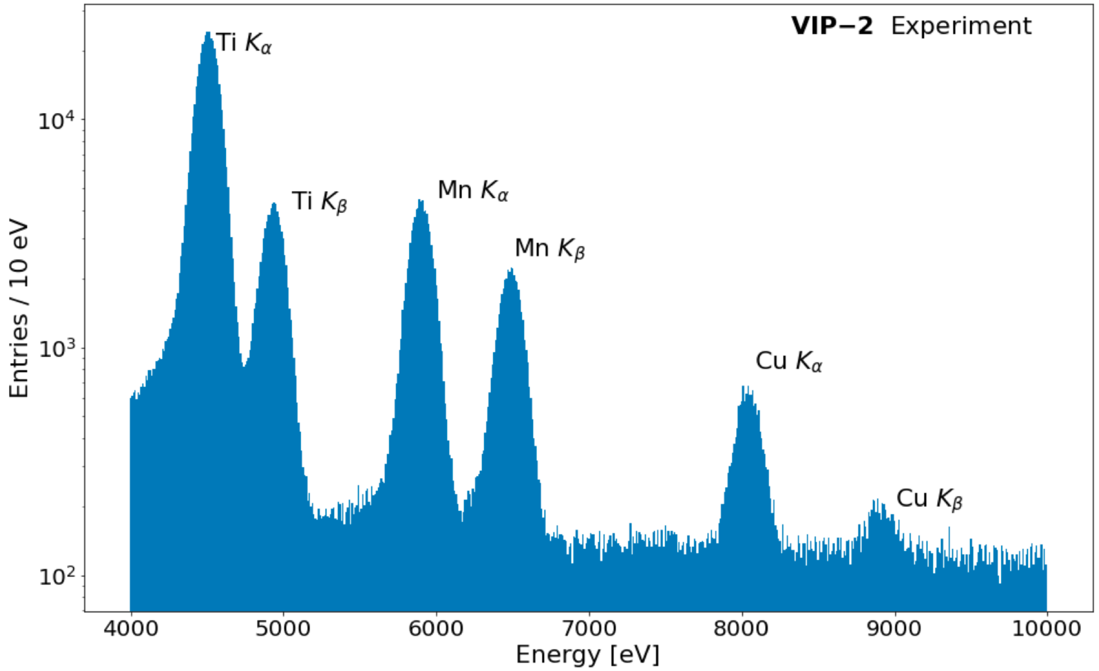

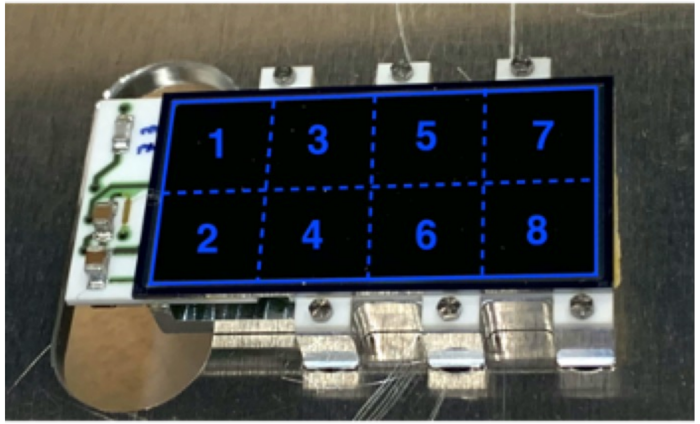

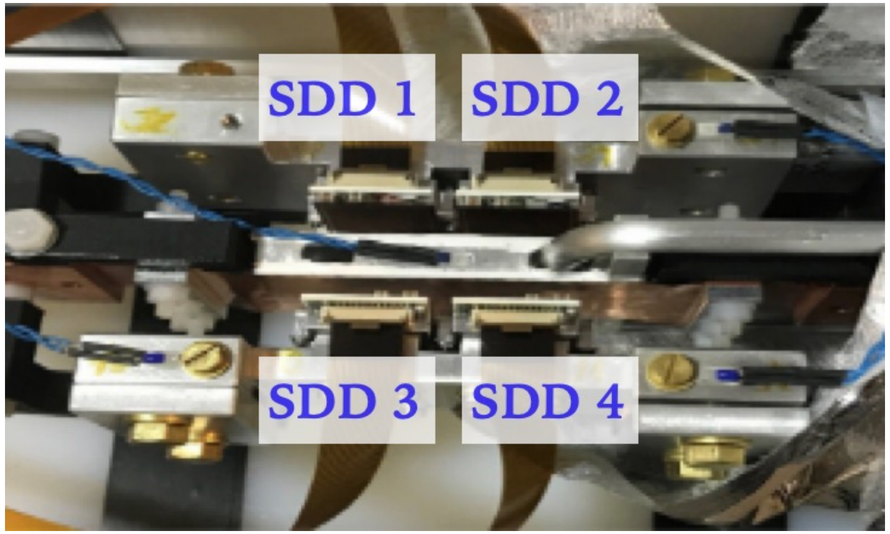

The VIP-2 Experiment

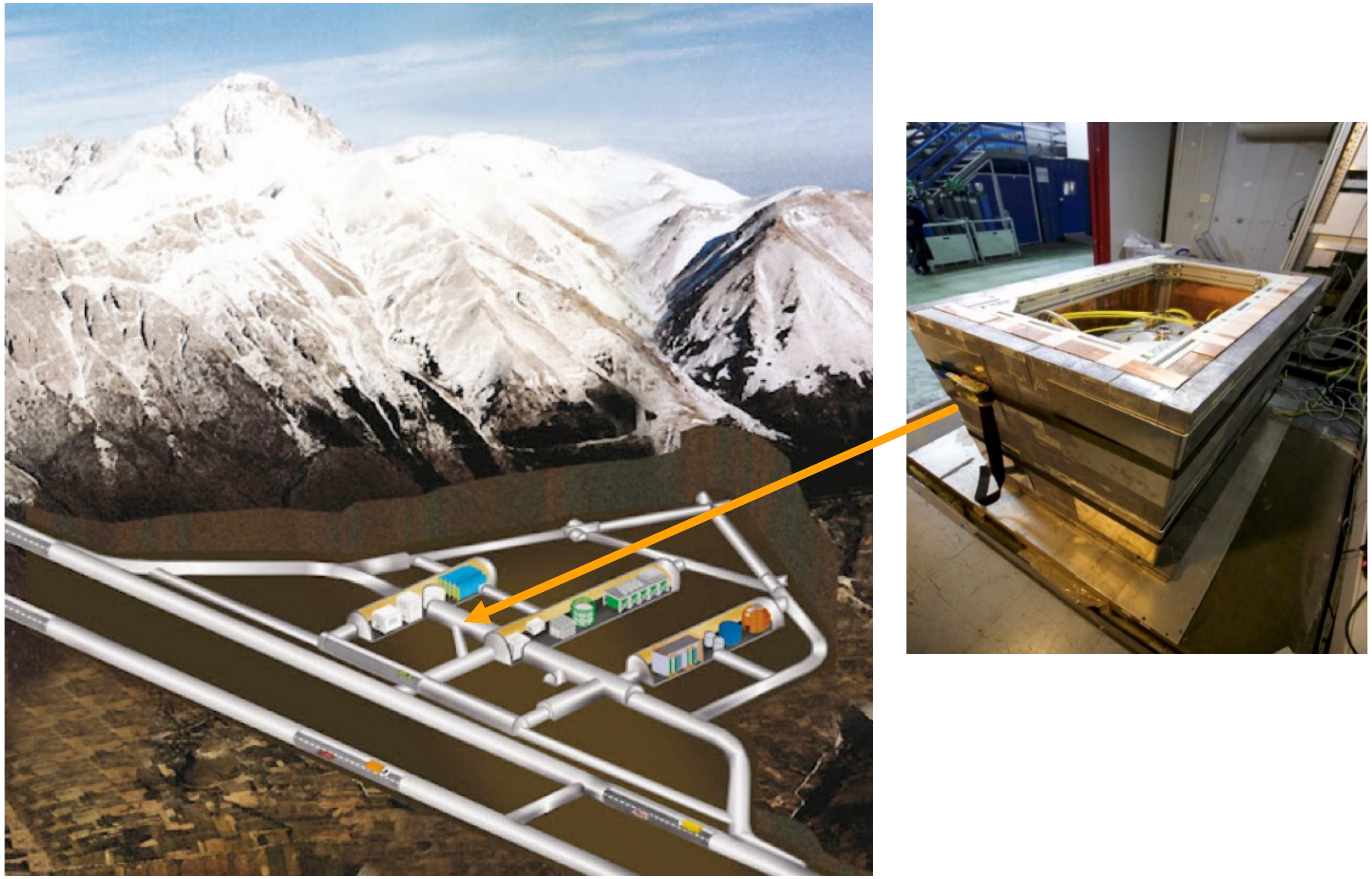

The experiment is performed in the low-background environment of the underground Gran Sasso National Laboratory of INFN:

● overburden corresponding to a minimum thickness of 3100 m w.e.

● the muon flux is reduced by almost six orders of magnitude, n flux of three orders of magnitudes.

● the main background source consists of γ-radiation produced by long-lived γ-emitting primordial isotopes and their decay products.

The VIP-2 Experiment

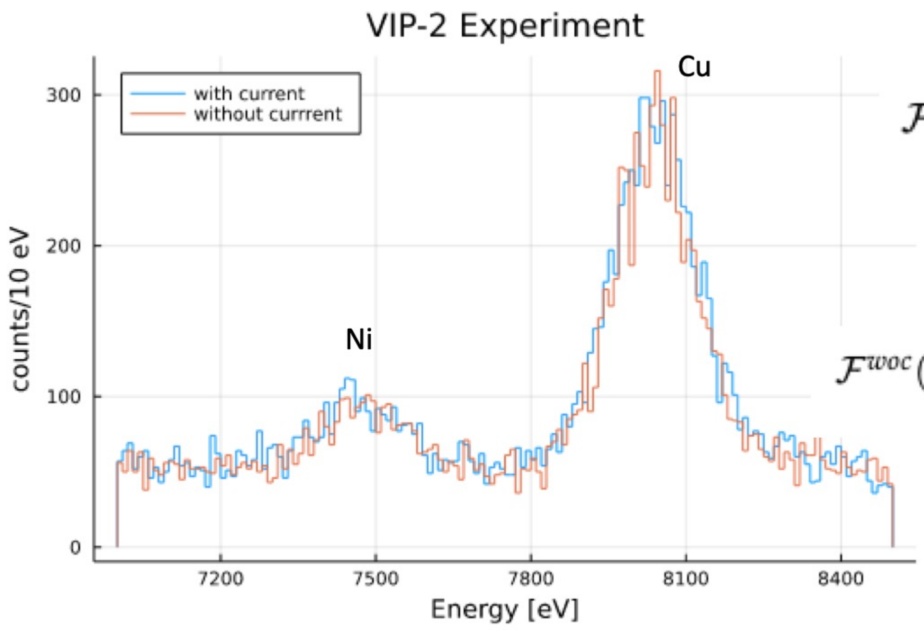

Description spectrum with current

Six months of data taking

$$\mathcal{F}^{wc}(\boldsymbol{\theta},\boldsymbol{y},\mathcal{S}) = y_1 \times Ni(\theta_1,\theta_2) + y_2 \times Cu(\theta_3,\theta_4) + + y_3 \times \mathrm{pol}_1(\theta_5) + \mathcal{S} \times PEPV(\theta_4)$$

Description spectrum without current

$$\mathcal{F}^{woc}(\boldsymbol{\theta},\boldsymbol{y}) = y_1 \times Ni(\theta_1,\theta_2) + y_2 \times Cu(\theta_3,\theta_4) + y_3 \times \mathrm{pol}_1(\theta_5)$$

Likelihood

$$\mathcal{L}(\mathcal{D}^{wc},\mathcal{D}^{woc}|\boldsymbol{\theta},\boldsymbol{y},\mathcal{S}) = \mathrm{Poiss}(\mathcal{D}^{wc}|\mathcal{F}^{wc}(\boldsymbol{\theta},\boldsymbol{y},\mathcal{S})) \times \mathrm{Poiss}(\mathcal{D}^{woc}|\mathcal{F}^{woc}(\boldsymbol{\theta},\boldsymbol{y} \times \mathcal{R}))$$

Bayesian

$$p(\boldsymbol{\theta},\boldsymbol{y},\mathcal{S}|\mathcal{D}^{wc},\mathcal{D}^{woc}) = = \frac{\mathcal{L}(\mathcal{D}^{wc},\mathcal{D}^{woc}|\boldsymbol{\theta},\boldsymbol{y},\mathcal{S})p(\boldsymbol{\theta},\boldsymbol{y},\mathcal{S})}{\int d\boldsymbol{\theta} d\boldsymbol{y} \mathcal{L}(\mathcal{D}^{wc},\mathcal{D}^{woc}|\boldsymbol{\theta},\boldsymbol{y},\mathcal{S})p(\boldsymbol{\theta},\boldsymbol{y},\mathcal{S})}.$$

Frequentist

$$t_{\mathcal{S}} = -2\ln\Lambda(\mathcal{S}) = -2\ln\frac{\mathcal{L}(\hat{\hat{\boldsymbol{\theta}}},\hat{\hat{\boldsymbol{y}}},\mathcal{S})}{\mathcal{L}(\hat{\boldsymbol{\theta}},\hat{\boldsymbol{y}},\hat{\mathcal{S}})}$$

$$p_{\mathcal{S}} = \int_{t_{obs}}^{\infty} f(t_{\mathcal{S}}|\mathcal{S})dt_{\mathcal{S}}$$

Symmetry **2022**, 14(5), 893;
https://doi.org/10.3390/sym14050893

The VIP-2 Experiment

Bayesian

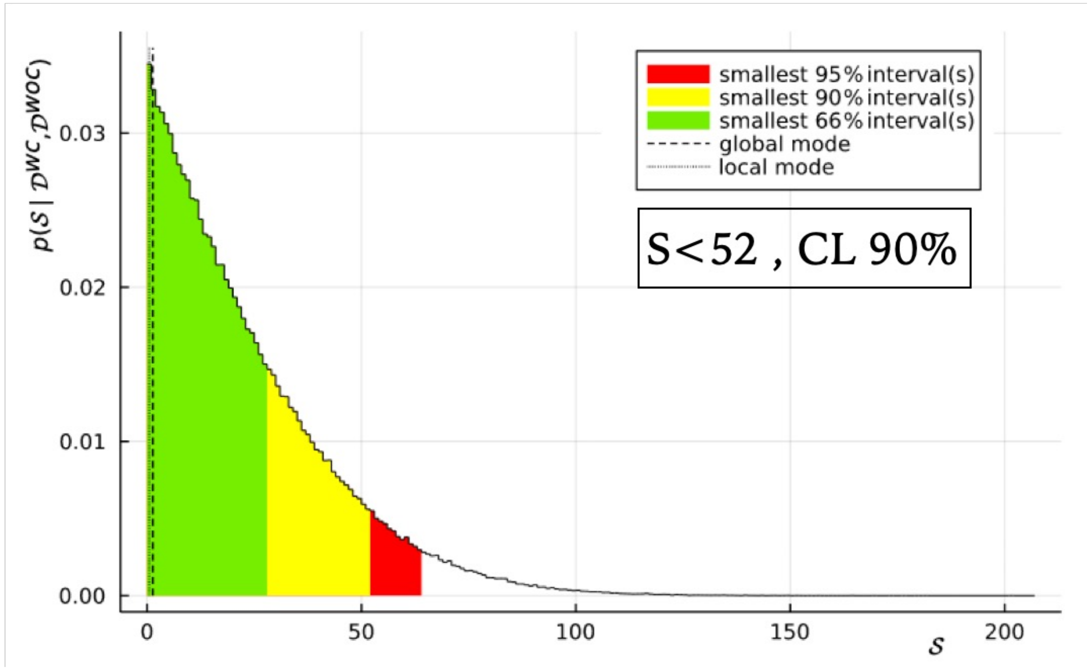

Frequentist

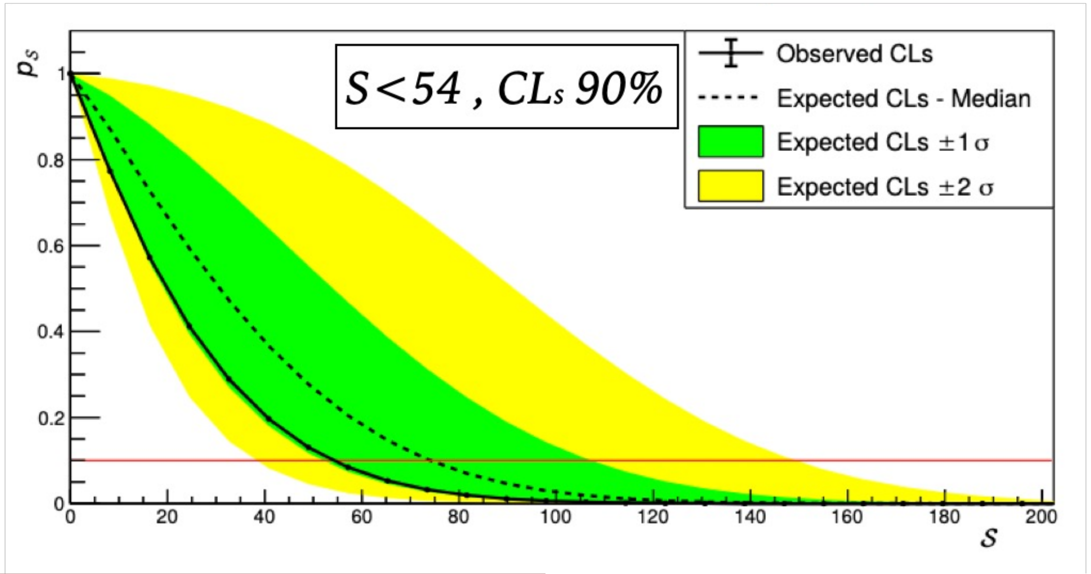

$$\Delta N_x \geq \frac{\beta^2}{2} N_{new} \frac{1}{10} N_{scatt} \times Eff_{riv}$$

$N_{int} = D/\mu$ → $\beta^2/2 \leq 8.6 \times 10^{-31}$ (Bayesian), $\beta^2/2 \leq 8.9 \times 10^{-31}$ (CL_s)

Random Walk → $\beta^2/2 \leq 6.8 \times 10^{-43}$ (Bayesian), $\beta^2/2 \leq 7.1 \times 10^{-43}$ (CL_s).

Symmetry **2022**, 14(5), 893;
https://doi.org/10.3390/sym14050893

The VIP-3 experiment – new SDDs

- New vacuum chamber to install 64 SDDs (1mm thick) :
  - ➢ Increased geometrical efficiency by a factor of 2 compared to VIP-2
  - ➢ Increased energy range: possibility to study the PEP in other elements (Ag, Sn, Pd)
- New front-end electronic for a better noise rejection and electrical stability
- New thermal contact between cold finger and SDDs
- New target cooling system → higher current up to 400 A

VIP-3

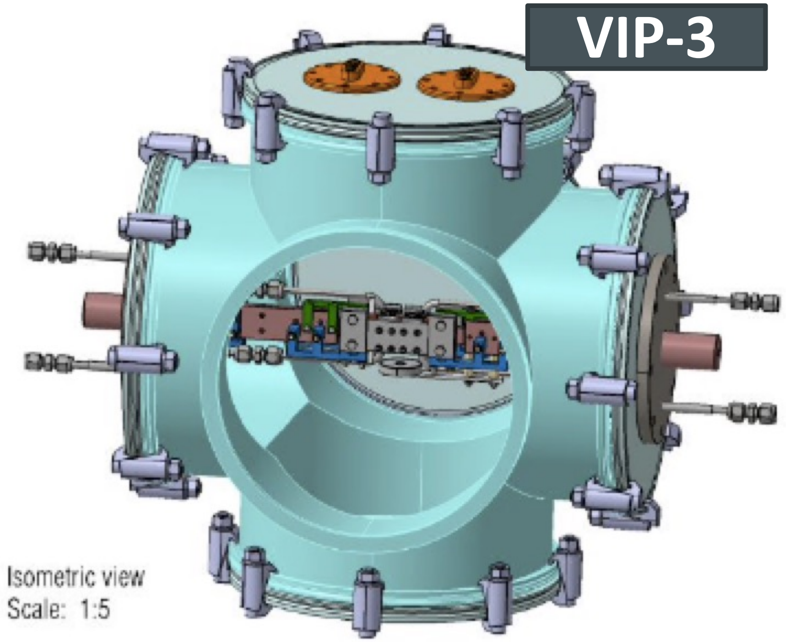

Higher quantum efficiency needed for the SDDs at higher Z:
use 1 mm thick SDDs, allowing to scan e.g. Ag, Sn and Pd

SDD 1mm

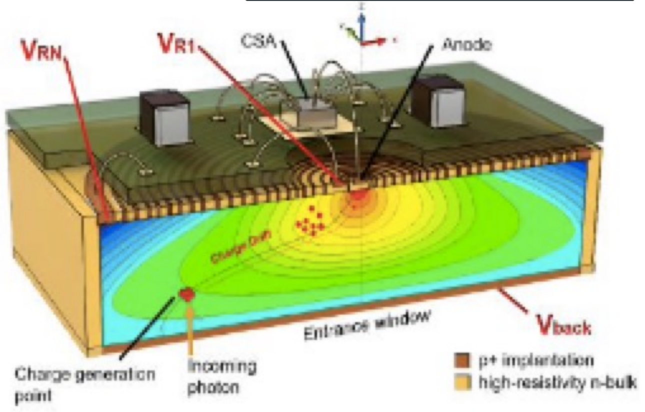

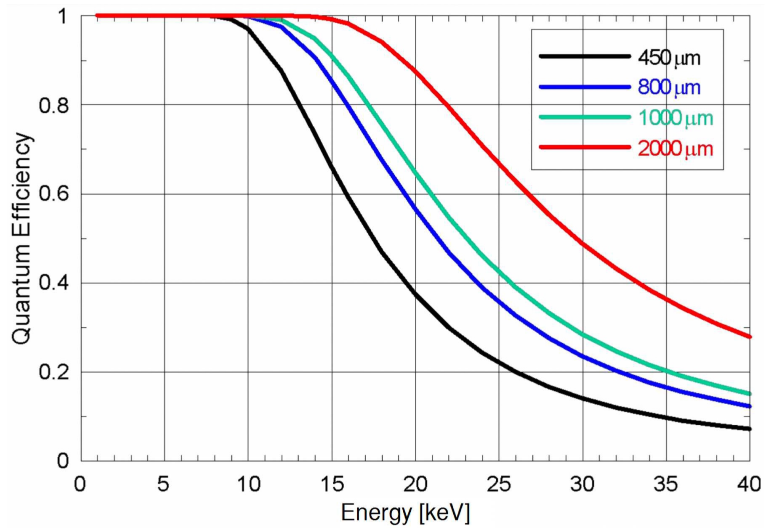

VIP-3: the new 1mm SDDs

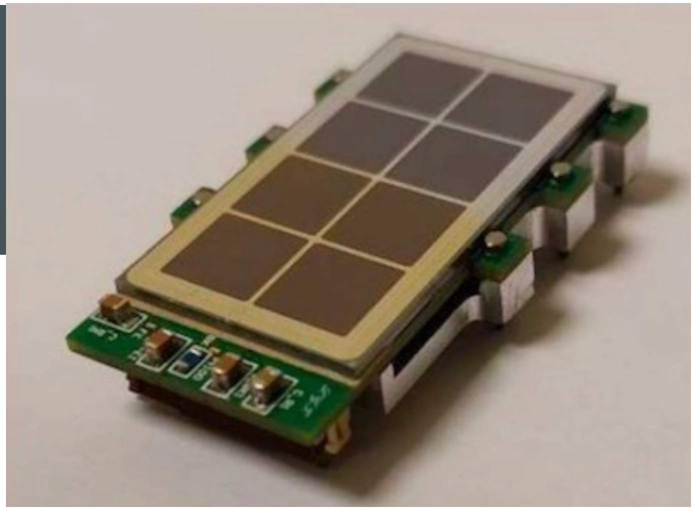

New 1mm thick SDDs have been developed by INFN in collaboration with FBK, SMI, PoliMi

- 8x8 mm^2 active area for each cell
- New Guard ring to avoid charge sharing between SDDs - preserve the energy and time resolution
- New PCB for noise reduction and electrical stability
- First prototype assembled and tested: FWHM ~140 eV @ 5.9 keV

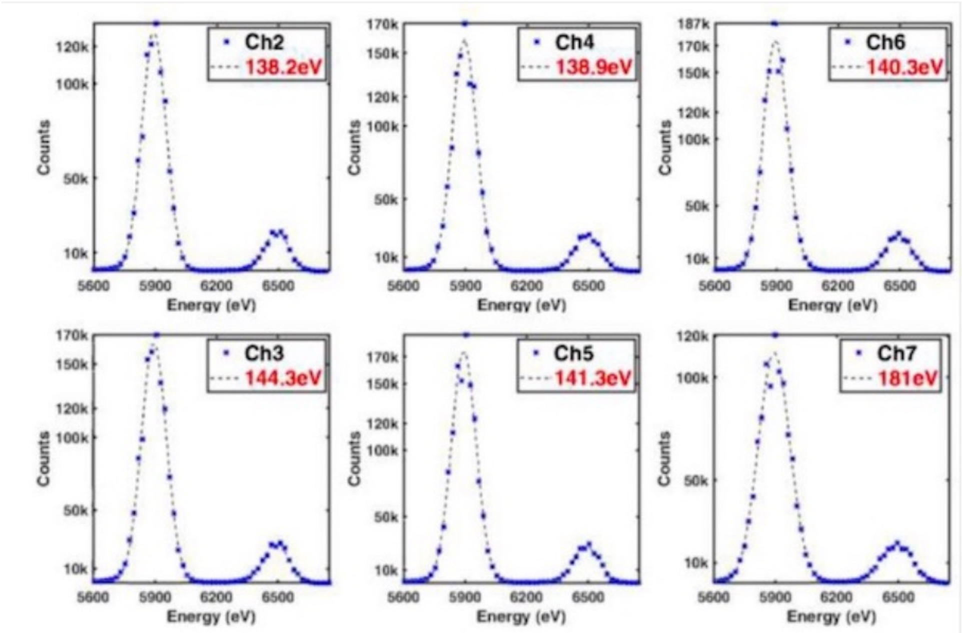

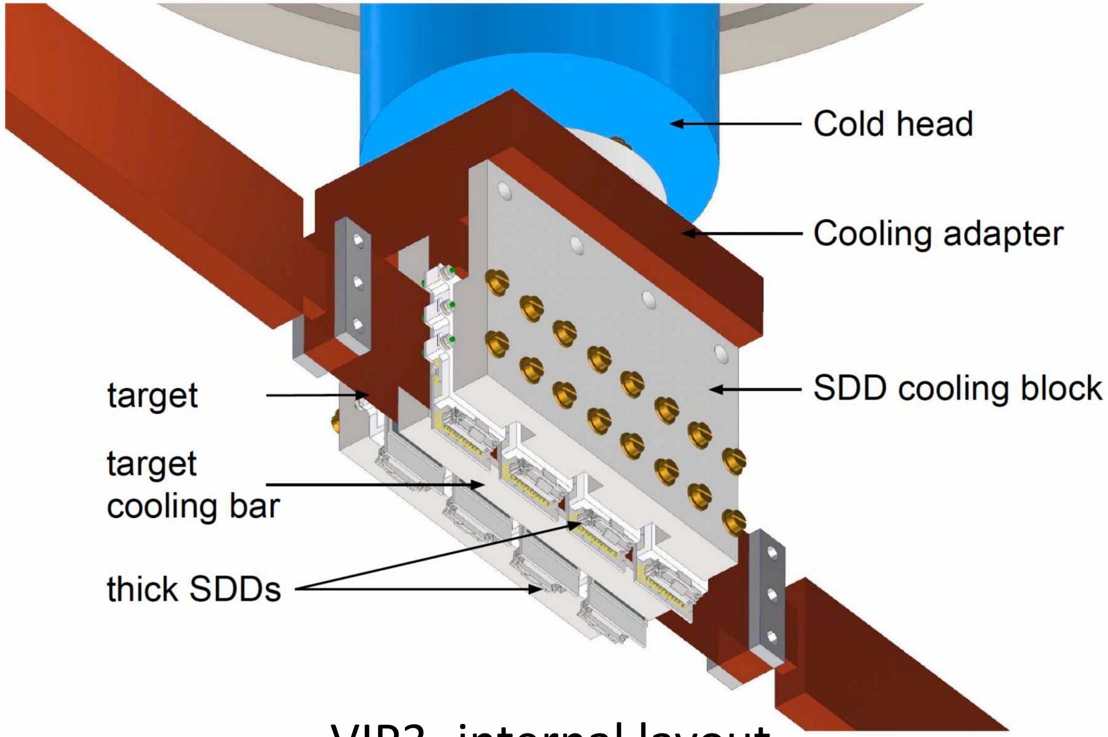

VIP3- internal layout

Conclusion

- Silicon Drift Detectors have been fully characterized:
  - **Linear energy response** within ± 3 eV (4–14 keV range) → $\delta E/E < 10^{-3}$ eV.
  - **Energy resolution** about 160 eV @ 140 K
  - **Stable energy response** within 1 eV.
  - **Timing resolution** about 360 ns @ 140 K

- **SDDs successfully employed to investigate the PEP**

$N_{int} = D/\mu$ → $\beta^2/2 \leq 8.6 \times 10^{-31}$ (Bayesian), $\beta^2/2 \leq 8.9 \times 10^{-31}$ (CL_s)

Random Walk → $\beta^2/2 \leq 6.8 \times 10^{-43}$ (Bayesian), $\beta^2/2 \leq 7.1 \times 10^{-43}$ (CL_s).

- **The VIP-3 setup is under construction → Larger active area, higher current, new generation of SDDs (1mm thick)**

Detectors for X-ray spectroscopy

SDDs
- 100 eV max resolution
- 4-40 keV range
- High efficiency

Cd(Zn)Te
- 20-300 keV range
- FWHM / E ~ %
- High efficiency
- Room Temperature

HPGe
- 100-1000 keV range
- FWHM / E ~ %
- High efficiency
- Cooling needed